Electrical characterization of RuO_x/*n*-GaN Schottky diodes formed by oxidizing ruthenium thin-films in normal laboratory air

Cite as: AIP Advances 10, 015116 (2020); doi: 10.1063/1.5125784
Submitted: 26 August 2019 • Accepted: 20 December 2019 •
Published Online: 8 January 2020

Noah Allen,[1] Timothy Ciarkowski,[2] Eric Carlson,[2] Amrita Chakraborty,[1] and Louis Guido[1,2,a)]

AFFILIATIONS

[1]Bradley Department of Electrical and Computer Engineering, Virginia Tech, Blacksburg, Virginia 24061, USA
[2]Department of Materials Science and Engineering, Virginia Tech, Blacksburg, Virginia 24061, USA

[a)]Author to whom correspondence should be addressed: louis.guido@vt.edu

ABSTRACT

Schottky diodes were formed by oxidizing Ru thin films deposited on *n*-type GaN at 400, 500, and 600 °C in normal laboratory air, and their electrical behavior was compared to that of a Ru/*n*-GaN reference device. The GaN epitaxial layers were grown via metalorganic chemical vapor deposition. The ruthenium films were deposited by electron beam evaporation. The Schottky barriers were characterized via current vs voltage (IV) and deep-level transient spectroscopy (DLTS) measurements between 70 and 400 K. The temperature dependent forward bias IV characteristics were fit, and the extracted temperature dependence of the effective barrier height for each device was shown to be caused by inhomogeneity at the metal/semiconductor interface. It was found that barrier inhomogeneity could be well described by a modified log-normal distribution. In reverse bias, it was shown that the low-energy tail of the barrier distribution is an important factor in determining leakage current. Favorable results occur for diodes oxidized at 400 and 500 °C, but raising the oxidation temperature to 600 °C results in a drastic increase in leakage current. DLTS measurements reveal one electron trap at $E_C - 0.57$ eV in each of the samples. It was found that the concentration of this 0.57 eV trap increases substantially at 600 °C and that trap-assisted tunneling likely contributes an additional pathway for reverse leakage current.

I. INTRODUCTION

Gallium nitride (GaN) has been examined with great interest for its implementation in both optical and high power semiconductor devices. Some of the properties that make GaN such an interesting material include a large direct bandgap (3.41 eV), low intrinsic carrier concentrations, high saturation-electron velocity, and high breakdown field strength. Ruthenium oxide[1–4] has been considered for making Schottky and ohmic contacts to various semiconductor devices because of its large work-function (>5.0 eV), low sheet resistance, high optical transparency, and good thermal stability. In the case of *p*-type GaN, ohmic contacts with specific contact resistivity in the range 10^{-5} to 10^{-6} Ω-cm^2 have been realized by depositing Ru/Pt[5] or Ru/Ni[6] metal bilayers and then annealing in nitrogen or oxygen, respectively. For *n*-type GaN, RuO_2 formed by reactive sputtering of a RuO_2 target has been employed to make Schottky diodes with large barrier height and low leakage current[7] and to form Schottky gate electrodes on AlGaN/GaN heterojunction field-effect transistors.[8] Alternatively, thin ruthenium layers deposited on *n*-GaN were annealed in oxygen to make transparent Schottky electrodes for use in metal-semiconductor-metal ultraviolet photodetectors.[9]

In the present work, RuO_x/*n*-GaN Schottky diodes were fabricated by depositing ruthenium metal on an *n*-type GaN epitaxial layer and then "oxidizing" this composite structure in normal laboratory air. The Schottky barriers so formed were characterized via current vs voltage (IV) and deep-level transient spectroscopy (DLTS) measurements between 70 and 400 K in addition to capacitance vs voltage (CV) measurements at room temperature. The experimental results are used to explain the inhomogeneous nature

of these Schottky barriers and to track changes in their behavior with oxidation temperature. Favorable results occur for diodes oxidized at 400 and 500 °C, but raising the oxidation temperature to 600 °C results in a substantial increase in leakage current. One detectable electron trap at E_C − 0.57 eV was identified in each of the samples, and it is speculated that trap-assisted tunneling contributes to reverse leakage current.

II. MATERIALS AND METHODS

Metal organic chemical vapor deposition (MOCVD) was employed to prepare two different GaN epitaxial layer structures on 2-in. diameter sapphire substrates. The first structure consists of a 1 μm thick, unintentionally doped (UID) GaN buffer layer having high electrical resistivity. This material was used to evaluate optical and electrical properties of Ru and RuO_x films. The second structure contains an identical UID GaN buffer layer followed by a 1 μm thick, silicon-doped GaN test layer. Hall-effect measurements at room temperature yield an electron density of 1.5×10^{17} cm^{-3} and carrier mobility of 568 cm^2/V s for the silicon-doped GaN layer. This material was utilized to form Ru/*n*-GaN and RuO_x/*n*-GaN Schottky diodes.

Thin ruthenium films (10 nm) were deposited by electron-beam evaporation and then oxidized to form RuO_x by annealing in normal laboratory air at 400, 500, or 600 °C for 5 min. Optical transmission measurements show that transparency (T) of the as-deposited Ru film is low over the entire visible and near ultraviolet spectrum (T at 380 nm = 31%). However, transparency of the RuO_x films increases with oxidation temperature (400, 500, and 600 °C anneals yield T at 380 nm of 37%, 46%, and 53%, respectively). Other workers have reported similar results with a near doubling of optical transparency between the as-deposited Ru and the best RuO_x film.[9] Electrical resistivity (ρ) of Ru and RuO_x films was obtained using the circular transfer length method. The as-deposited Ru film has the highest value of $\rho = 2.4 \times 10^{-4}$ Ω-cm, but a substantial reduction to $\rho = 7.1 \times 10^{-5}$ Ω-cm is achieved via oxidation at 400 °C. Nonetheless, raising the oxidation temperature further gives rise to an increase in electrical resistivity (500 and 600 °C anneals yield $\rho = 9.3 \times 10^{-5}$ and 1.3×10^{-4} Ω-cm, respectively). These results are in the range of electrical resistivity reported by others for thicker RuO_2 films made by reactive sputtering[2,3] or thermal annealing.[4]

The Ru/*n*-GaN and RuO_x/*n*-GaN Schottky diodes were fabricated using conventional photolithographic techniques. First, the UID GaN/*n*-GaN material structure was divided into four samples which were cleaned at room-temperature in acetone, IPA, aqua regia, and 49% HF, with each step performed for 10 min and then followed by thorough rinsing in de-ionized water. Next, a photoresist mask was patterned to expose openings for the top-surface ohmic contacts, and then the samples were dipped in 10:1 BOE, rinsed in de-ionized water, dried with nitrogen, and immediately placed in the electron-beam evaporator. Ohmic contacts consisting of Ti/Al (30 nm/400 nm) were deposited, patterned via photoresist lift-off, and then annealed in forming gas at 600 °C for 5 min. Following the same procedures, ruthenium Schottky contacts with a thickness of 10 nm were deposited and patterned into circles with diameters varying between 200 and 450 μm. Three RuO_x/*n*-GaN Schottky diode samples were prepared using the ruthenium oxidation procedure outlined above. For the fourth sample, the ruthenium film was retained in its as-deposited state to provide Ru/*n*-GaN reference devices. Finally, contact pads of Ni/Ag (50 nm/300 nm) were deposited on both ohmic and Schottky contacts yielding 144 diodes on each sample.

All viable devices on each of the four samples were characterized via IV measurements at room-temperature using a Keithley 2400 source-measure unit (SMU). Additionally, CV measurements were taken at room-temperature using an HP4192A impedance analyzer with a 1 MHz probing signal mixed with a dc voltage swept from zero-bias to −5 V. The results of these measurements were used to screen out anomalous devices and to identify diodes having well-behaved forward and reverse IV curves. The extracted device parameters are listed in Table I. The barrier heights and ideality factors shown here are on par with those reported in the literature,[7–10] especially given the variety of RuO_x deposition methods, film thicknesses, and annealing conditions. Note that all ideality factors exceed unity and the CV barriers are consistently higher than those obtained from IV data (the same is true in previous reports[7,10]). Both of these findings suggest the possibility of inhomogeneous metal/semiconductor (M/S) interfaces,[11] and as such, it would be more appropriate if the barrier height distribution was compared.

One point of departure for the present work is the electron density in the *n*-GaN layer. The values obtained via CV are consistent with Hall-effect data from the unprocessed UID GaN/*n*-GaN epitaxial structure. Moreover, the electron density does not change as a consequence of the ruthenium oxidation process ($n \approx 1.4 \times 10^{17}$ cm^{-3} for all three annealing temperatures). In contrast, Lee *et al.*[7] reported a nearly 10× reduction in electron density ($n \approx 3.04 \rightarrow 0.45 \times 10^{16}$ cm^{-3}) after annealing RuO_2/*n*-GaN Schottky contacts at 500 °C in nitrogen for 30 min. In that case, the 40 nm RuO_2 film was prepared by RF magnetron sputtering. Additionally, Ramesh *et al.*[10] showed $1/C^2$ vs voltage plots in which the slope of the fitting lines continued to increase with annealing temperature (indicating

TABLE I. Schottky diode parameters at 300 K extracted using IV and CV measurements. Average values and standard deviations from over 100 devices on each of the four processed samples are given.

Method	Parameter	As-deposited	Oxidized (400 °C)	Oxidized (500 °C)	Oxidized (600 °C)
IV measurements at 300 K	Barrier height (eV)	0.83 ± 0.05	1.09 ± 0.05	1.02 ± 0.10	0.88 ± 0.02
	Ideality factor	1.09 ± 0.02	1.22 ± 0.07	1.19 ± 0.17	1.10 ± 0.02
CV measurements at 300 K	Barrier height (eV)	0.95 ± 0.05	1.33 ± 0.07	1.31 ± 0.07	1.14 ± 0.06
	Electron density (10^{17} cm^{-3})	1.4 ± 0.2	1.4 ± 0.2	1.4 ± 0.2	1.4 ± 0.2

a reduction in electron density from the initial value of $n \approx 4.07 \times 10^{17}$ cm^{-3}). Those RuO_x/n-GaN Schottky contacts were made using 50 nm Ru films deposited via electron-beam evaporation and then annealed over the temperature range 300–500 °C in nitrogen for 1 min.

Upon completion of the device screening and evaluation process described above, one Ru/n-GaN diode and three RuO_x/n-GaN diodes, i.e., one diode from each processed sample, with a Schottky electrode diameter of 400 μm were selected to perform variable-temperature IV (IVT) and DLTS measurements. Electrical data were recorded between 70 and 400 K with a Keithley 2400 SMU and SULA fast capacitance meter, respectively. Temperature control and sample probing were achieved using a modified MMR cryogenic vacuum chamber.

III. EXPERIMENTAL RESULTS

Current vs voltage measurements of the four preselected Schottky diodes were first performed at 300 K under both forward and reverse bias conditions. In Fig. 1, the semilogarithmic IV characteristics are shown for the as-deposited, 400, 500, and 600 °C oxidized devices. In an ideal Schottky diode, the IV relationship is governed by thermionic emission (TE) over a voltage independent barrier, and the current as a function of applied voltage (V_A) is given by[13]

$$I(V_A) = AA^*T^2 \exp\left(\frac{-q\phi_{b0}}{k_BT}\right)\left[\exp\left(\frac{q(V_A - IR_s)}{\eta k_BT}\right) - 1\right], \quad (1)$$

where A is the M/S interface area, A^* is the Richardson constant of GaN (26.4 A/cm^2 K^2[14]), ϕ_{b_o} is the zero-bias barrier height, η is the ideality factor, and R_S is the series resistance. Experimental values of zero-bias barrier height and ideality factor can be extracted from the forward IV characteristics according to Eq. (1), but careful consideration must be given to the current or voltage range used so as not to include series resistance effects.

While methods for Schottky diode parameter extraction have been developed,[15–17] it was found that accurate fitting to experimental data could be achieved by entering the zero-bias barrier height, ideality factor, and series resistance as input parameters to an iterative fitting procedure based on Eq. (1). By utilizing the Levenberg-Marquardt dampened least-squares iterative fitting algorithm, experimental data could be accurately fit with coefficient of determination (R^2) values greater than 0.999 across the full voltage range. Diode parameters extracted in this manner are summarized in Table II.

TABLE II. Device parameters extracted from IV measurements at 300 K for the four preselected Schottky diodes.

Sample	ϕ_{b_o} (eV)	η	R_s (Ω)	J_R at −10 V (μA/cm^2)
As-deposited	0.89	1.06	79.6	56
Oxidized (400 °C)	0.95	1.11	133.5	3.2
Oxidized (500 °C)	0.99	1.12	66.6	0.8
Oxidized (600 °C)	0.86	1.06	51.6	240

Oxidizing ruthenium metal in air to form RuO_x/n-GaN Schottky diodes has a considerable effect on both forward and reverse IV characteristics, as shown in Fig. 1 and Table II. In the forward bias regime, the extracted values of barrier height are 0.89, 0.95, 0.99, and 0.89 eV and the ideality factors are 1.06, 1.11, 1.12, and 1.06 for the as-deposited, 400, 500, and 600 °C oxidized samples, respectively. Werner and Guttler[11] showed that ideality factors in excess of unity indicate the presence of inhomogeneity at the M/S interface. In reverse bias, the leakage current densities (J_R) are 56, 3.2, 0.8, and 240 μA/cm^2 at −10 V for the as-deposited, 400, 500, and 600 °C oxidized samples, respectively. It is notable that J_R at −10 V for the 500 °C oxidized sample approaches the lowest value reported to date for RuO_2/n-GaN Schottky diodes (Lee *et al.* reported J_R at −10 V of 0.6 μA/cm^2 in Ref. 7). However, the voltage dependence of J_R cannot be accounted for by assuming thermionic emission over a homogeneous M/S barrier.

In order to learn more about the nature of the M/S interfaces in these Ru/n-GaN and RuO_x/n-GaN Schottky diodes, variable temperature IV measurements were performed between 70 and 400 K (in steps of 4 K) on the same devices used in Fig. 1. Once

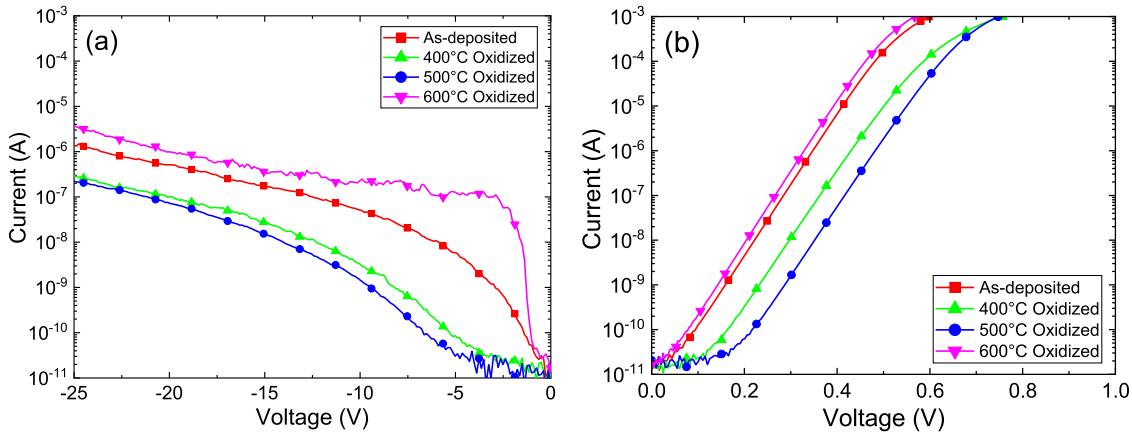

FIG. 1. Room-temperature reverse (a) and forward (b) IV curves for as-deposited, 400, 500, and 600 °C oxidized devices.

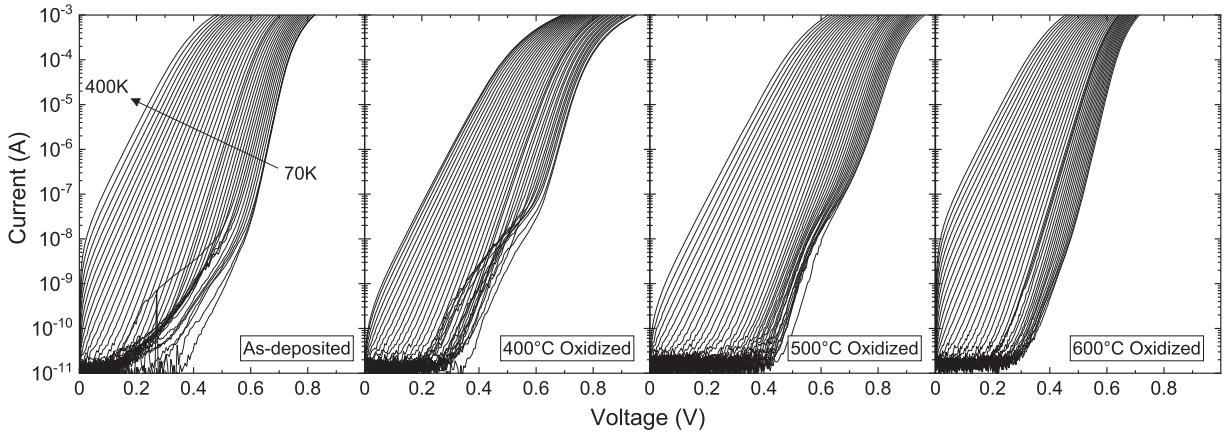

FIG. 2. Forward IV characteristics for as-deposited, 400, 500, and 600 °C oxidized devices measured from 70 to 400 K.

temperature was stabilized within ±100 mK for >30 s, a Keithley 2400 SMU was used to measure the IV characteristics shown in Fig. 2.

In addition to the linear region predicted by Eq. (1), and the roll-over in the high-current range caused by series resistance, each of the four samples exhibits a second linear region, pronounced at temperatures below 150 K and at low currents. The presence of this additional region is assumed to stem from isolated variation at the M/S interface which presents as a small area parallel Schottky diode in the IVT characteristics.[18] Therefore, in order to employ the previously mentioned iterative fitting method of parameter extraction, a multidiode model of the form given by Eq. (2) is necessary. Here, the variables $\phi_{b_i}^{eff}(0,T)$, η_i, and R_{s_i} are the temperature-dependent zero-bias effective barrier height, ideality factor, and series resistance of the i-th diode, respectively,

$$I(V_A) = AA^*T^2 \sum_{i=1}^{n} \exp\left(\frac{-q\phi_{b_i}^{eff}(0,T)}{kT}\right)\left[\exp\left(\frac{q(V_A - IR_{s_i})}{\eta_i k_B T}\right) - 1\right]. \tag{2}$$

In the present case, a two-diode model is used, for each of the four samples, such that n is 2 in Eq. (2) for temperatures where this additional linear region is present in the IVT data. Fitting the IVT

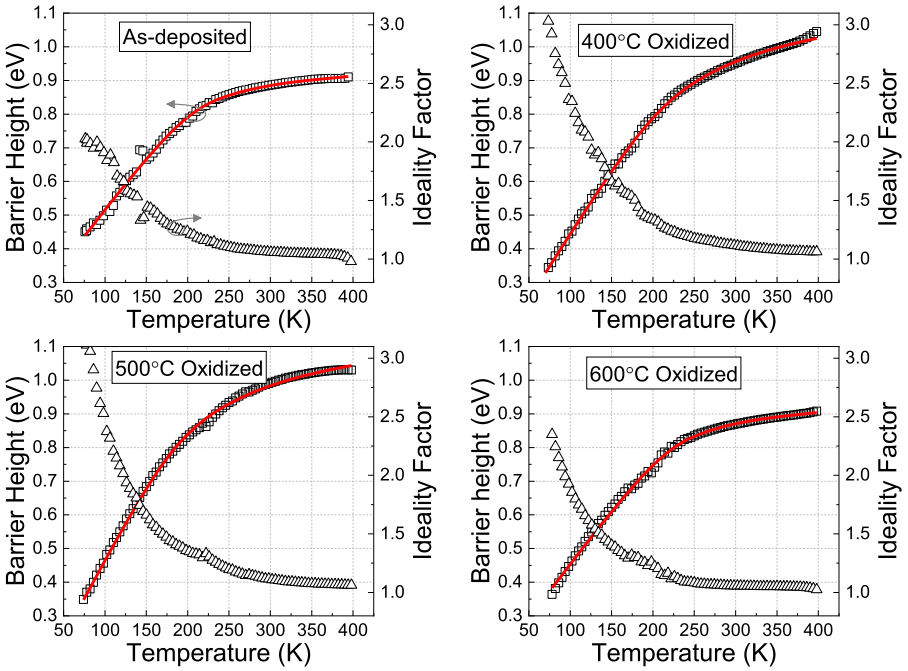

FIG. 3. Extracted zero-bias barrier heights (□) and ideality factors (Δ) from 70 to 400 K for as-deposited, 400, 500, and 600 °C oxidized devices. The solid red lines represent best fits to experimental barrier heights utilizing the modified log-normal distribution inhomogeneity model.

characteristics across the full voltage and current range resulted in R^2 values larger than 0.999 for all four samples. The extracted values of the zero-bias effective barrier height and ideality factor outside of the low current linear region are plotted vs measurement temperature in Fig. 3. The existence of temperature dependence for both the ideality factor and zero-bias effective barrier height confirms the likelihood of barrier height inhomogeneity at the M/S interface. From Fig. 3, it can be seen that the effective zero-bias barrier height of each diode increases with temperature and begins to roll-over for measurements taken at T > 225 K. Additionally, the extracted values of the ideality factor decrease with temperature and approach unity, indicative of a homogeneous-like interface at higher temperatures.

In order to understand how oxidizing Ru/*n*-GaN samples to form RuO_x/*n*-GaN Schottky diodes impacts the GaN layer near the surface of the epitaxial material, DLTS was performed on the same devices used for IVT characterization. DLTS measurements were made from 70 to 400 K in steps of 2 K. Deep levels were probed with a steady-state bias of −5 V and a 1 ms zero-bias filling pulse after which 300 ms of the capacitance transient was recorded. The DLTS spectra calculated at an emission rate of 23.9 Hz for each sample are shown in Fig. 4.

One detectable electron trap is present in each of the samples as evidenced by the single peak in the DLTS spectra. Trap activation energies (E_T) and capture cross sections (σ) were extracted from Arrhenius plots of the emission rate data between 6 and 400 s^{-1} following the method introduced by Lang.[19] Trap concentrations (N_T) were calculated according to the following equation, where ΔC is the change in capacitance from the initial value $C(0)$ to the steady-state value (C_∞) and N_D is the free electron concentration:

$$N_T = 2\frac{\Delta C}{C_\infty}N_D. \tag{3}$$

The trap characteristics are summarized in Table III. Trap energies differ slightly and the capture cross sections vary between 5.4 and 12.8 × 10^{-16} cm^2, but these signatures are likely attributable to the same ubiquitous GaN electron trap located ~0.57 eV below the conduction band. Previously, the concentration of the 0.57 eV trap level was linked to various impurity species,[20–22] growth substrate,[23–25] and extrinsic perturbations.[26,27] The recent work by Galiano *et al.*[28] was able to spatially link the signal from this trap to pure edge dislocations and possible interactions with impurities.

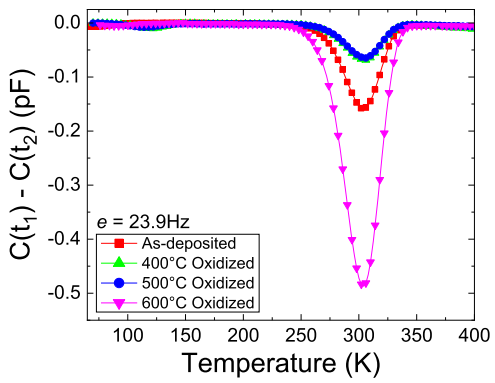

FIG. 4. DLTS spectra for as-deposited, 400, 500, and 600 °C oxidized devices.

TABLE III. Electron trap characteristics in GaN for as-deposited, 400, 500, and 600 °C oxidized devices.

Sample	E_T (eV)	σ (10^{-16} cm^2)	N_T (10^{15} cm^{-3})
As-deposited	0.58	5.39	1.91
Oxidized (400 °C)	0.59	8.68	1.04
Oxidized (500 °C)	0.60	12.8	0.89
Oxidized (600 °C)	0.57	6.53	5.47

IV. ANALYSIS AND DISCUSSION

Schottky diode barrier inhomogeneity models were developed previously which rely on describing the interface as a continuous distribution of barriers.[11,12,29,30] Plotting the effective barrier height vs $(2k_BT)^{-1}$ yields neither a single nor a multilinear trend; thus, the models outlined by Werner and Guttler,[11] Song *et al.*,[12] and Chand and Kumar[29] are not appropriate to explain the barrier height temperature dependence. Iterative analysis according to the model proposed by Jiang *et al.*[30] produced disagreement with effective barrier heights extracted above 200 K. Recently, Allen *et al.*[18] demonstrated that interface barrier inhomogeneity both at zero bias and under simulated forward biases can be well described by a modified log-normal distribution. In this approach, the temperature dependence of the effective barrier height is defined as follows:

$$\phi_b^{eff}(V,T) = -\frac{k_BT}{q}\ln\left(\int_{-\infty}^{\infty} P\left(\phi_b^V\right)\exp\left(\frac{-q\phi_b^V}{k_BT}\right)d\phi_b^V\right). \tag{4}$$

Here, the experimentally determined zero-bias barrier heights, $\phi_b^{eff}(0,T)$, become a function of a probabilistic barrier height distribution, $P\left(\phi_b^V\right)$. The modified log-normal distribution used to describe the experimental data is given by Eq. (5). Fitting the temperature-dependent effective barrier height data is accomplished by iteratively solving Eq. (4) while adjusting the parameters, *A*, *B*, and *C*, and the lower limit of integration, to minimize the sum of squares error. Using the lower limit of integration as an iteratively varied parameter better estimates the form of the lower energy portion of the barrier distribution. The best-fit temperature dependent effective barrier height curves are plotted as solid red lines in Fig. 3. Additionally, the modified log-normal distributions which produced these curve fits are shown in Fig. 5,

$$P\left(\phi_b^V\right) = \frac{1}{C(-\phi_b^V + A)\sqrt{2\pi}}\exp\left(-\frac{\left[\ln\left(-\phi_b^V + A\right) - B\right]^2}{2C^2}\right). \tag{5}$$

The excellent agreement between the measured temperature dependence of the zero-bias effective barrier heights and the fitting curves shown in Fig. 3 demonstrates that the inhomogeneity at these M/S interfaces can be characterized by the modified log-normal distributions in Fig. 5. According to Eq. (4), it is the low energy tail of the barrier distributions that should have the greatest impact on effective barrier heights, and in turn on Schottky diode IV characteristics. The inset of Fig. 5 magnifies the low energy tail of each

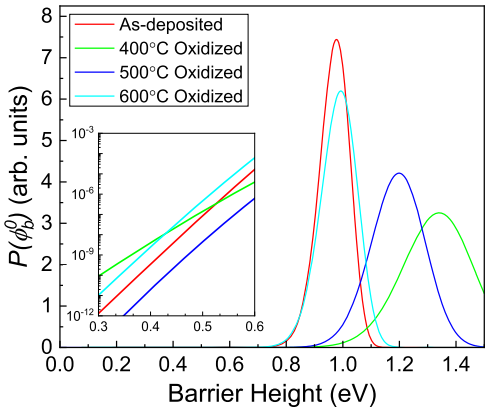

FIG. 5. Modified log-normal distributions which best fit zero-bias effective barrier height data extracted from IVT measurements for as-deposited, 400, 500, and 600 °C oxidized devices. The inset accentuates the low energy tail of each barrier distribution.

barrier distribution. Additionally, calculated distributions could be compared with those of similarly prepared diodes reported within the literature. However, this work is the first description detailing the IV temperature dependence of as-deposited and annealed ruthenium contacts to GaN, and thus, direct comparison cannot be made to Refs. 7–10.

With the form of the inhomogeneity at the M/S interface having been established, it is now possible to consider its impact on reverse leakage current [i.e., the IV curves plotted in Fig. 1(a)]. Assuming the reverse current is dominated by TE, reducing the magnitude of the low energy tail of the barrier height distribution should reduce leakage current.

Comparing probability distributions in Fig. 5, a large increase in barrier height occurs between as-deposited and 400 °C oxidized diodes. The peak barrier height increases from 0.96 to 1.34 eV, while the distribution also broadens considerably. Others showed that as-deposited Ru films are polycrystalline with a columnar grain structure and a work function of around 4.6 eV.[4,9] Thermal annealing at 400 °C in a mixed O_2/N_2 (1/20) ambient for 30 min forms RuO_2 on the outer surfaces of the Ru grains.[4] Ruthenium oxide in direct contact with *n*-GaN should give rise to an increase in barrier height given the significant increase in work function (the work function of RuO_2 formed by thermal oxidation was shown to be around 5.1 eV[4]). Kim and Lee[9] reported RuO_2/*n*-GaN Schottky barriers in the range 1.33–1.43 eV for RuO_2 electrodes formed via thermal oxidation. Examination of the inset in Fig. 5, however, reveals that the diode oxidized at 400 °C also exhibits an increase in the density of barriers lower than 0.53 eV (relative to the as-deposited sample). *This increase in the proportion of low energy barriers should lead to an increase in leakage current, which is not supported by the IV curves shown in* Fig. 1(a).

Raising the Ru oxidation temperature to 500 °C causes the peak of the barrier height distribution to shift downward from 1.34 to 1.2 eV. At this temperature, the oxidized ruthenium film should contain a larger proportion of RuO_2, but it is also possible that volatile RuO_4 was formed leaving patches of the *n*-GaN surface bare.[31] Then, deposition of Ni/Ag contact pads would create a spatially varying M/S interface with some combination of RuO_2/*n*-GaN and Ni/*n*-GaN patches. The composite Schottky barrier would likely have a lower peak barrier height, consistent with the data shown in Fig. 5. Note, moreover, that the probability distribution for the 500 °C oxidized diode narrows, resulting in the smallest proportion of low energy barriers (inset of Fig. 5). This change in the Schottky barrier structure gives rise to the lowest reverse leakage current among all of the diodes. Oxidizing ruthenium at 600 °C should cause more extensive RO_4 formation giving rise to a larger area of the exposed *n*-GaN surface, which, upon Ni/Ag contact pad deposition, leads to an M/S interface containing mostly Ni/*n*-GaN regions. As a consequence, the peak barrier height is reduced to 0.98 eV, the low energy tail of the probability distribution becomes more substantial, and the leakage current takes on its highest value.

One shortcoming of this attempt to connect reverse leakage currents to pure TE over the low energy tail of inhomogeneous barrier height distributions is that it fails to explain the behavior of the 400 °C oxidized device. Moreover, it ignores the variation in concentration of the 0.57 eV electron trap and its possible contribution to leakage current. In fact, the trend in reverse leakage current for the set of Schottky diodes considered herein follows exactly the change in 0.57 eV trap concentration. This raises the possibility that electron tunneling through a continuum of trap states within the bandgap is the dominant mechanism for leakage current.[32,33]

The open question is what is the physical origin of the 0.57 eV trap states and how is their concentration influenced by device processing. It is well established that electron beam deposition of ruthenium on GaN introduces point defects near the M/S interface having energy levels inside the bandgap.[34] This could explain the high leakage current for the as-deposited Ru/*n*-GaN Schottky diode. Furthermore, these point defects may be "annealed out" of the GaN near surface region during the 400 and 500 °C ruthenium oxidation processes. Upon annealing at an even higher temperature (600 °C), it is possible that Ru and/or O atoms cluster near threading dislocations, thereby reintroducing 0.57 eV trap states from another physical source. This results in the high leakage current observed in Fig. 1(a) for the 600 °C oxidized diode. Nevertheless, the net donor concentration ($N_d - N_a$) is not significantly impacted by $N_T \approx 5 \times 10^{15}$ cm^{-3}, as evidenced by CV depth profiling (Table I), because the Si doping concentration is in excess of 10^{17} atoms/cm^3.

V. SUMMARY AND CONCLUSION

Schottky diodes were formed by oxidizing Ru thin films deposited on *n*-type GaN at 400, 500, and 600 °C in normal laboratory air, and their electrical behavior was compared to that of a Ru/*n*-GaN reference device. The temperature dependent forward bias IV characteristics were fit, and the extracted temperature dependence of the effective barrier height for each device was shown to be caused by inhomogeneity at the M/S interface. It was found that barrier inhomogeneity could be well described by a modified log-normal distribution. In reverse bias, it was shown that the low-energy tail of the barrier distribution is an important factor in determining leakage current. Favorable results occur for diodes oxidized at 400 and 500 °C, but raising the oxidation temperature to 600 °C results in a drastic increase in leakage current. DLTS measurements reveal one electron trap at $E_C - 0.57$ eV in each of the samples. It was found that the concentration of this 0.57 eV trap increases

substantially at 600 °C and that trap-assisted tunneling likely contributes an additional pathway for reverse leakage current.

ACKNOWLEDGMENTS

L.J.G. would like to acknowledge The Bradley Department of Electrical and Computer Engineering at Virginia Tech for operating and maintaining the Micron Technology Semiconductor Processing Lab. L.J.G. would also like to thank the MSE Department at Virginia Tech for its continuous support. N.P.A. is grateful for funding support from the Bradley Graduate Fellowship provided by The Bradley Department of Electrical and Computer Engineering at Virginia Tech. This research was funded by the ARPA-E SWITCHES program under Grant No. DE-AR0000446, monitored by program managers Dr. T. Heidel and Dr. I. Kizilyalli.

REFERENCES

[1] L. F. Mattheiss, Phys. Rev. B **13**, 2433 (1976).
[2] L. Krusinelbaum and M. Wittmer, J. Electrochem. Soc. **135**, 2610 (1988).
[3] E. Kolawa, F. C. T. So, W. Flick, X. A. Zhao, E. T. S. Pan, and M. A. Nicolet, Thin Solid Films **173**, 217 (1989).
[4] E. Jelenkovic and K. Y. Tong, J. Vac. Sci. Technol., B **22**, 2319 (2004).
[5] J. S. Jang, S. J. Park, and T. Y. Seong, Appl. Phys. Lett. **76**, 2898 (2000).
[6] H. W. Jang, W. Urbanek, M. C. Yoo, and J.-L. Lee, Appl. Phys. Lett. **80**, 2937 (2002).
[7] S. H. Lee, J. K. Chun, J. J. Hur, J. S. Lee, G. H. Rue, and Y. H. Bae, IEEE Electron Dev. Lett. **21**, 261 (2000).
[8] S. H. Hahm, Y. H. Lee, M. B. Lee, and J. H. Lee, Proc. IEEE **1-2**, 1280 (2001).
[9] J. K. Kim and J. L. Lee, J. Electrochem. Soc. **151**, G190 (2004).
[10] C. K. Ramesh, V. R. Reddy, and K. S. R. K. Rao, J. Mater. Sci.: Mater. Electron. **17**, 999 (2006).
[11] J. H. Werner and H. H. Guttler, J. Appl. Phys. **69**, 1522 (1991).
[12] Y. P. Song, R. L. Van Meirhaeghe, W. H. Laflère, and F. Cardon, Solid-State Electron. **29**, 633 (1986).
[13] E. H. Rhoderick and R. H. Williams, *Metal-Semiconductor Contacts*, 2nd ed. (Oxford Science Publications, 1988).
[14] M. R. H. Khan, T. Detchprohm, P. Hacke, K. Hiramatsu, and N. Sawaki, J. Phys. D: Appl. Phys. **28**, 1169 (1995).
[15] J. H. Werner, Appl. Phys. A: Mater. Sci. Process. **47**, 291 (1988).
[16] H. Norde, J. Appl. Phys. **50**, 5052 (1979).
[17] S. K. Cheung and N. W. Cheung, Appl. Phys. Lett. **49**, 85 (1986).
[18] N. Allen, T. Ciarkowski, E. Carlson, and L. Guido, Semicond. Sci. Technol. **34**, 095003 (2019).
[19] D. V. Lang, J. Appl. Phys. **45**, 3023 (1974).
[20] D. W. Cardwell, A. Sasikumar, A. R. Arehart, S. W. Kaun, J. Lu, and S. Keller, Appl. Phys. Lett. **102**, 193509 (2013).
[21] A. Armstrong, A. R. Arehart, D. Green, U. K. Mishra, J. S. Speck, and S. A. Ringel, J. Appl. Phys. **98**, 053704 (2005).
[22] H. K. Cho, C. S. Kim, and C. H. Hong, J. Appl. Phys. **94**, 1485 (2003).
[23] P. Hacke, T. Detchprohm, K. Hiramatsu, N. Sawaki, K. Tadatomo, and K. Miyake, J. Appl. Phys. **76**, 304 (1994).
[24] Y. Tokuda, Y. Matsuoka, H. Ueda, O. Ishiguro, N. Soejima, and T. Kachi, Superlattices Microstruct. **40**, 268 (2006).
[25] Z. Q. Fang, D. C. Look, P. Visconti, D. F. Wang, C. Z. Lu, and F. Yun, Appl. Phys. Lett. **78**, 2178 (2001).
[26] W. Nakamura, Y. Tokuda, H. Ueda, and T. Kachi, Physica B **376**, 516 (2006).
[27] S. A. Goodman, F. D. Auret, F. K. Koschnick, J. M. Spaeth, B. Beaumont, and P. Gibart, Mater. Sci. Eng.: B **71**, 100 (2000).
[28] K. Galiano, J. I. Deitz, S. D. Carnevale, D. A. Gleason, P. K. Paul, and Z. Zhang, J. Appl. Phys. **123**, 224504 (2018).
[29] S. Chand and J. Kumar, Semicond. Sci. Technol. **11**, 1203 (1996).
[30] Y. L. Jiang, G. P. Ru, F. Lu, and X. P. Qu, Chin. Phys. Lett. **19**, 553 (2002).
[31] S. H. Oh, C. G. Park, and C. Park, Thin Solid Films **359**, 118 (2000).
[32] Y. Lei, H. Lu, D. Cao, D. Chen, R. Zhang, and Y. Zheng, Solid-State Electron. **82**, 63 (2013).
[33] E. J. Miller, E. T. Yu, P. Waltereit, and J. S. Speck, Appl. Phys. Lett. **84**, 535 (2004).
[34] F. D. Auret, S. A. Goodman, G. Myburg, F. K. Koschnick, J.-M. Spaeth, B. Beaumont, and P. Gibart, Physica B **273-274**, 84 (1999).